Journal of Cellular Biochemistry 98:1629–1644 (2006)

Modulation of Mouse RANKL Gene Expression by Runx2 and PKA Pathway

Kiyoshi Mori,[1] Riko Kitazawa,[1] Takeshi Kondo,[1] Sakan Maeda,[1] Akira Yamaguchi,[2] and Sohei Kitazawa[1]*

[1]Department of Bioinformatics, Division of Molecular Pathology,
Kobe University Graduate School of Medicine, 7-5-1 Kusunoki-cho, Chuo-ku, Kobe 650-0017, Japan
[2]Department of Oral Restitution, Section of Oral Pathology, Graduate School of Tokyo Medical and Dental University, 1-5-45 Yushima, Bunkyo-ku, Tokyo 113-8549, Japan

Abstract Runx2 regulates the target genes characteristic of osteoblastic phenotypes, while exerting diverse and sometimes controversial effects on osteoblastic cells depending on their differentiation stage. Receptor activator of nuclear factor-κB (RANK) ligand (RANKL) is a membrane bound cytokine essential for osteo(chondro)clastogenesis. During endochondral ossification, while Runx2-positive hypertrophic chondrocytes express RANKL, the steady-state expression of the *RANKL* gene in osteoblastic cells is, at later stages, kept at a relatively low level to sustain the established bone. The aim of this study was to elucidate the mechanism whereby Runx2 and the protein kinase A (PKA) pathway modulate RANKL expression, especially from the viewpoint of their functions in RANKL basic promoter activity and in chromatin structural changes in osteoblastic/stromal cells. Osteoblastic/stromal cell lines derived from normal and Runx2-deficient mice were used to analyze endogenous RANKL gene expression by real-time reverse transcription (RT)-PCR, the acetylation status of the H3 and H4 histone proteins associated with the 5′-flanking region of the *RANKL* gene by chromatin immunoprecipitation, and the exogenously transfected RANKL gene promoter activity both in the steady-state and under PKA-activated conditions. Here, we demonstrate that Runx2 suppresses steady-state RANKL gene expression by condensing chromatin, while showing a slightly positive effect on RANKL basic promoter activity. Besides acting through the CRE-like region (−0.96 kb) of the RANKL gene promoter, forskolin (FK) treatment transactivates the *RANKL* gene by antagonizing the function of Runx2, by reducing Runx2 mRNA expression and by opening the chromatin conformation far upstream (more than 40 kb) of the *RANKL* gene. J. Cell. Biochem. 98: 1629–1644, 2006.

Key words: RANKL; Runx2; PKA; chromatin remodeling; gene promoter

Bone formation and resorption are maintained and regulated by two types of cells, osteoblasts and osteoclasts [Ducy et al., 2000; Teitelbaum, 2000]. Various bone-seeking inter- and intra-cellular signals including hormones, cytokines, enzymes, minerals, and transcription factors are known to modulate bone mass by controlling the proliferation, differentiation, and function of these two types of cells.

Osteoclasts are multinucleated giant cells involved in resorbing mineralized tissues Suda et al., 1999; Boyle et al., 2003; Teitelbaum and Ross, 2003]. The membrane-bound factor expressed on osteoblastic/stromal cells has been postulated to be an essential factor for the differentiation and maintenance of osteoclasts based on the observation that the direct contact between cells of the monocyte/macrophage lineage and osteoblastic/stromal cells is essential for in vitro osteoclastogenesis in the mouse co-culture system [Takahashi et al., 1988; Udagawa et al., 1989]. This factor has been isolated and identified as a membrane-bound ligand for a cytokine receptor, receptor activator of nuclear factor-κB ligand (RANKL) [Lacy et al., 1998; Yasuda et al., 1998]. It is now

Grant sponsor: Ministry of Education, Culture, Sports, Science and Technology of Japan; Grant numbers: 16590278, 16590313.

*Correspondence to: Sohei Kitazawa, Division of Molecular Pathology, Kobe University Graduate School of Medicine, 7-5-1 Kusunoki-cho, Chuo-ku, Kobe 650-0017, Japan.
E-mail: kitazawa@med.kobe-u.ac.jp

Received 8 November 2005; Accepted 17 January 2006
DOI 10.1002/jcb.20891

widely accepted that, besides the suppression of functional RANKL by a soluble decoy receptor, osteoprotegerin (OPG), the interaction between RANKL and its cognate receptor, receptor activator of nuclear factor-κB (RANK), expressed on the surface of osteoclast precursors, triggers osteoclastic differentiation [Nakagawa et al., 1998]. So far, at least four different pathways are known to modulate osteoclastogenesis through RANKL expression in osteoblasts: $1\alpha,25(OH)_2D_3$ (VitD), cyclic AMP-protein kinase A (PKA), interleukin 6 (IL-6)/IL-11-glycoprotein 130 (gp130), and calcium ion-protein kinase C (PKC) [Takami et al., 2000].

On the other hand, osteoblasts are bone-forming cells originating from undifferentiated skeletal mesenchymal cells [Yamaguchi et al., 2000]. A striking phenotype of the lack of mineralized bone in Runt-related gene 2 (*Runx2*)-knockout animals clearly shows that *Runx2* is a master gene for the commitment, proliferation, and differentiation of the osteoblastic cell lineage [Ducy et al., 1997; Komori et al., 1997; Otto et al., 1997]. Runx2, a member of the transcription factors homologous to the *Drosophilla* protein, runt [Kania et al., 1990], acquires enhanced DNA-binding activity when it heterodimerizes with core binding factor β (Cbfb) [Yoshida et al., 2002]. At the initial stage of osteoblast differentiation, this heterodimer, together with the recently identified osterix, a transcription factor downstream of Runx2, regulates the expression of target genes that define osteoblastic phenotypic characterization such as bone sialoprotein, type I collagen, and osteocalcin [Kern et al., 2001; Roca et al., 2005; Xiao et al., 2005]. At a late stage, however, Runx2 also suppresses the differentiation of osteoblastic cells [Liu et al., 2001; Geoffroy et al., 2002].

Putative Runx2-binding sites are located in the *RANKL* gene basic promoter region, suggesting that Runx2 is involved in osteoblast-specific RANKL gene expression [Kitazawa et al., 1999]. Indeed, Runx2-deficient mice completely lack osteoclasts, and RANKL expression is severely diminished in such mice [Komori et al., 1997]. Conversely, O'Brien et al. [2002] have reported that Runx2 is capable of binding to the RANKL gene promoter without affecting *RANKL* gene activity in osteoblastic/stromal cells. It is recently reported that Runx2 is not essential for VitD-modulated RANKL gene expression in osteoblastic cells because high-dose VitD treatment induces osteoclast-like tartrate-resistant acid phosphatase (TRACP)-positive multinucleated cells in the coculture of C6 cells, derived from the calvaria of Runx2-deficient mice, with normal mouse bone marrow macrophages (BMM) [Notoya et al., 2004].

In this study, to clarify the precise role of Runx2 and the PKA pathway in RANKL expression, especially from the viewpoint of the function of Runx2 in the basic promoter region of the *RANKL* gene and of chromatin structural changes in osteoblastic/stromal cells, we investigated the role of Runx2 on RANKL gene expression both in the steady-state and under PKA-activated conditions using osteoblastic/stromal cell lines derived from normal and Runx2-deficient mice. Here, we demonstrate that Runx2 suppresses steady-state RANKL gene expression by condensing chromatin, while showing a slightly positive effect on the basic promoter activity of the *RANKL* gene. FK treatment antagonizes the function of Runx2 by reducing Runx2 mRNA expression and by opening the chromatin conformation far upstream (more than 40 kb) of the *RANKL* gene.

MATERIALS AND METHODS

Cell Lines, Cell Culture, and In Vitro Osteoclast-Like Cell Formation

Mouse bone marrow stromal cell line ST2 and Runx2−/− mouse-derived mesenchymal cell line C6 were cultured in α-MEM (Sigma, St. Louis, MO) supplemented with 10% FBS (Sigma), 100 μg/ml penicillin/streptomycin (ICN Biomedicals, Inc., Aurora, OH) and 125 mM L-glutamine (ICN Biomedicals, Inc.), and maintained at 37°C in a humidified atmosphere with 5% CO_2. ST2 or C6 cells were co-cultured with mouse BMM isolated from the femora and tibiae of 8-week-old male mice [Kitazawa et al., 1995] for 7 days with or without 10^{-8} M or 10^{-7} M of $1\alpha(OH)_2D_3$ (VitD) (Chugai Pharmaceutical Co., Ltd., Tokyo, Japan) and/or 10^{-8} M of dexamethasone (Dex) (Sigma), or 10^{-5} M of forskolin (FK) (Wako Pure Chemical Industries, Ltd., Osaka, Japan). TRACP staining was conducted with a commercial kit (Sigma) and the number of osteoclast-like TRACP-positive multinucleated (>3 nuclei) cells was counted.

Plasmid Construction

The 5′-flanking region of the mouse *RANKL* gene was cloned as described previously

[Kitazawa et al., 1999], and the 2 kb upstream from the transcription start site was ligated into a pGL3 Basic vector (Promega, Madison, WI) resulting in a pGL3-2k vector. Nested deletion mutants were ligated into the pGL3 vector, then pGL3-1005 and pGL3-723 were generated, as previously described [Kitazawa and Kitazawa, 2002]. Constructs with mutated Runx2-binding site(s) (Runx2-1: AACCTCA (−368/−362) to AACCTTG, Runx2-2: AACCACT (−207/−201) to AACCTTG and Runx2-3: AACCCACA (−194/−187) to AACCCTTG) or mutated CRE (mutCRE: TGAGGTCA (−969/−962) to TGAGGAGG) were generated by recombinant PCR strategy as previously described [Kitazawa and Kitazawa, 2002]. Mutated PCR products were ligated into the pGL3-Basic vector, resulting in pGL3-mutRunx2-2, pGL3-mutRunx2-2,3, pGL3-mutRunx2-1,2,3, and pGL3-mutCRE. These constructs were transfected into ST2 or C6 cells using LipofectAMINE (Invitrogen, Carlsbad, CA). The phRG-TK vector (Promega) was co-transfected to standardize transfection efficiency. The cultured transfected cells were treated with 10 μM of FK and/or 3 μM of H89 (Seikagaku Corp., Tokyo, Japan) or the vehicle for 6 h, at which point they were lysed and subjected to dual luciferase assay (Promega) with an ATP-3010 luminometer (Advantech, Tokyo, Japan).

Generation of Runx2-Expressing Vector and Stable Tet-On C6 Cell Line

Mouse Runx2 cDNA derived from pKSαA1 kindly gifted by Dr. Yoshiaki Ito (Institute of Molecular Cell Biology, Singapore) [Ogawa et al., 1993] were cloned into the *Xho*I/*Bam*HI site of the pTRE2hyg vector (Clontech, Palo Alto, CA) to generate doxycycline (Dox)-responsible Runx2 expressing vector pTRE2hyg-Runx2. The pTet-On-puro vector containing the puromycin resistance gene was generated (the puromycin resistance gene was ligated into the *Xho*I site of the pTet-On vector (Clontech)), as a regulatory vector.

C6 cells at 70% confluence were transfected with 6 μg of the pTet-On-puro vector using LipofectAMINE and plated in 6-cm culture dishes (Becton Dickinson Labware, Franklin Lakes, NJ) at a density of 2.0×10^5/plate. Clones selected with 2 μg/ml puromycin (Clontech) treatment were isolated by cloning cylinders (IWAKI, Tokyo, Japan) and subcloned. Dox-responsive C6 cell lines were selected by transient transfection with the pTRE2hyg-Luc vector (Clontech) and luciferase assay.

Stable pTet-On-puro transfected C6 cells (C6-12IA7F) at 70% confluence in 10-cm culture dishes (Becton Dickinson Labware) were transiently transfected with the pTRE2hyg-Runx2 vector using LipofectAMINE (Invitrogen). After a 6-h interval, the cells were treated with 1 μg/ml of Dox (Sigma). Runx2 mRNA and protein expression were confirmed by reverse transcription (RT)-PCR and immunoblotting, respectively. Transfected cells cultured in DMEM supplemented with 10% FBS were treated with 10 μM of FK for 24 h, and RNA was extracted for quantitative real-time RT-PCR.

RNA Extraction, Reverse Transcription (RT), and Quantitative Real-Time RT-PCR

One microgram of RNA isolated from each cell was reverse transcribed to produce cDNA, which was then amplified and quantified by the ABI PRISM 7300 Real Time PCR system (Applied Biosystems, Foster City, CA) using a set of primers and probes (Assay ID; Runx2, Mm00501578_m1, RANKL, Mm00441908_m1, OPG, Mm00435452_m1, activating transcription factor-4 (ATF-4), Mm00515324_m1, histone deacetylase 3 (HDAC3), Mm00515916_m1) (Applied Biosystems). For standardization of relative mRNA expression, rodent GAPDH primers and a probe (Assay ID; Mm99999915 g1) (Applied Biosystems) were used. Conventional RT-PCR was also conducted using 1 μg of total RNA and the following set of Runx2 and GAPDH primers: Runx2 (sense): 5′-ATGCGTATTCCTGTAGATCCG-3′, Runx2 (antisense): 5′-TTGGGGAGGATTTGTGAAGAC-3′, GAPDH (sense): 5′-TGCACCACCAACTGCTTAG-3′, GAPDH (antisense): 5′-GGATGCAGGGATGATGTTC-3′.

The results of cycle threshold values (Ct values) were calculated by the $\Delta\Delta C_t$ method to obtain the fold differences.

Electrophoretic Gel Motility Shift Assay (EMSA)

Nuclear extracts were prepared from ST2 cells as previously described [Kondo et al., 2004]. For EMSA, the following double-stranded oligonucleotides spanning the putative Runx2 binding sites (−378/−354, −214/−194, −200/−180) were used: Runx2-1 (−378/−354): 5′-CTGAGGCTAAACCTCACGATTCTTG-3′, Runx2-2 (−214/−194): 5′-AGAA ACCAACCACTGGACCC-3′, Runx2-3 (−200/

−180): 5′-GGACCCAACCCACAGCCTCCA-3′. Oligonucleotides were annealed and 5′-end-labeled with γ^{32}P-ATP (3,000 Ci/mmol) by T4 polynucleotide kinase (Promega, Madison, WI). The binding reaction was carried out by preincubating labeled oligonucleotides with nuclear extracts and a specific antibody against Runx2 (Santa Cruz Biotechnology, Inc., Santa Cruz, CA) at room temperature for 30 min. For the competition assay, 5-, 25-, and 125-fold molar excess amounts of unlabeled oligonucleotide containing two consensus Runx2-binding elements [Ducy et al., 1997], 5′-CAGAAACCAACCACAGGACCCAAACCACA-GCCTCCAC-3′, were added to the binding reaction. The reaction products were analyzed on a 5% polyacrylamide gel, electrophoresed at room temperature in 0.5× TBE buffer at 100 V for 3 h, then the gel was dried and analyzed with image analyzer BAS-EWS 4075 (FUJIX, Tokyo, Japan).

Immunoblotting

After transfection with pTRE2hyg-Runx2, C6-12IA7F cells were treated with Dox (1 μg/ml) for 24 h in 10-cm culture dishes, lysed by incubation at 4°C for 30 min in 2 ml of lysis buffer (20 mM sodium phosphate [pH7.0], 250 mM NaCl, 30 mM sodium pyrophosphate, 0.1% NP-40, 5 mM EDTA, 10 mM NaF, 0.1 mM Na_3VO_4) with 1 mM phenylmethyl sulfonyl fluoride (PMSF) and complete, Mini proteinase inhibitor cocktail tablet (Roche Diagnostics, Mannheim, Germany). The cell lysates were sonicated twice for 20 s at 40 kHz on ice, centrifuged at 12,500*g* for 30 min at 4°C, and the supernatants were stored at −80°C. Equal amounts of protein were separated by SDS–PAGE, electrotransferred to nitrocellulose membrane (Trans-Blot) from Bio-Rad laboratories (Hercules, CA), and immunoblotted with a primary antibody against Runx2 (Alpha Diagnostic International). Immunocomplexes were detected with the enhanced chemiluminescence (ECL) kit and Hyperfilm ECL (Amersham Biosciences, Piscataway, NJ).

RNA Interference Experiment

The RNA molecule (small interfering RNA (siRNA)) against Runx2 was synthesized by Ambion (Austin, TX), with the target mRNA sequences of sense: 5′-CGAUCUGAGAUUU-GUGGGCTT-3′, antisense: 5′-GCCCACAAAU-CUCAGAUCGTT-3′. ST2 cells were transfected with the siRNA using Silencer^{TM} siRNA Transfection Kit II (Ambion). As a control, non-specific siRNA (contained in the commercial kit) was transfected. After 48 h, total RNA was extracted for quantitative real-time RT-PCR.

Chromatin Immunoprecipitation (ChIP) Assay

Soluble chromatin was, according to the manufacturer's instructions (Upstate Biotechnology, Lakeplacid, NY), prepared from 1.0×10^6 cells fixed with formaldehyde, precleared with salmon sperm DNA/protein A agarose-50% slurry (Upstate), then 2 ml of the supernatant solution was incubated with anti-acetyl-Histone H3 antibody, anti-acetyl-Histone H4 antibody, or anti-phosphorylated Histone H3 (Ser 10) antibody overnight at 4°C with rotation. Immunoprecipitates were collected after salmon sperm DNA/protein A agarose-50% slurry treatment for 1 h at 4°C with rotation, and then washed according to the manufacturer's instructions. From eluted immunoprecipitates, DNA was recovered by phenol/chloroform extraction and ethanol precipitation and resuspended with 30 μl of 1× TE. Two microliters of DNA solution was used as a template for PCR. Four sets of primers for post-immunoprecipitated DNA amplification were designed. One set of primers was set as far as −40 kb upstream of the RANKL gene transcription start site (−40.3 kb), and three (−26.6, −12.7, and −0.95/−0.68 kb) were set to cover the region within 1 kb downstream of the CRE site (−26.7 kb) or the CRE-like regions (−12.8 and −0.96 kb). These sites were predicted according to the registered 5′-flanking sequence of the RANKL in the bacterial artificial chromosome (BAC) clone (No. PR23-189K24). For PCR amplification, the following sets of primers were used: RANKL-40.3K-S (sense): 5′-CTCCAG-GCCTTGAGTTGAC-3′; RANKL-40.3K-A (antisense): 5′-AGGTGATTTGATTCTGGGAAC-3′; RANKL-26.6K-S (sense): 5′-TGGAACTGGAG-TTACAGCTG-3′; RANKL-26.6-A (antisense): 5′-AAACTGATGTAGTCGGAATC-3′; RANKL-12.7K-S (sense): 5′-ATGATCAGGTTGAGTA-AGGATGC-3; RANKL-12.7K-A (antisense): 5′-GGACATATATGGAAACTCCAGC-3′; RANKL-0.95K-S (sense): 5′-GTTTGAGGTCAGCCTGG-TTCATATAG-3′; RANKL-0.68K-A (antisense): 5′-GCCTCACTGCTTAAGAAATCCTTATGC-3′.

Statistical Analysis

Data are expressed as means ± SEM. Statistical analyses were performed by Student's

t-test. The level of significance was taken to be $P < 0.05$.

RESULTS

Effect of FK on RANKL, OPG, and Runx2 Expression and on Osteoclastogenesis

The effect of FK on RANKL, OPG, and Runx2 mRNA expression was assessed by quantitative real-time RT-PCR using total RNA extracted from ST2 and C6 cells. In ST2 cells, while the level of RANKL expression in the steady state remained low, FK treatment (10^{-5} M) for 12 h resulted in an 86.6-fold increase in RANKL mRNA expression. Surprisingly, Runx2-deficient C6 cells expressed a high level (a 149-fold of the steady-state RANKL mRNA expression in ST2 cells) of RANKL mRNA in the steady-state condition, which resulted in a further 14-fold increase by FK treatment (Fig. 1A, left). On the other hand, OPG expression in C6 cells was threefold higher than in ST2 cells in the steady state, and FK treatment decreased its expression in both ST2 and C6 cells by 79.1% and 76.6%, respectively (Fig. 1A, middle). In ST2 cells, FK decreased Runx2 expression to 59% of the basal expression, while C6 cells did not express Runx2. To address the issue of whether reciprocal regulation of RANKL and OPG expression in ST2 and C6 cells by FK was functional, we assessed the capability of these cells for supporting osteoclastogenesis in a co-culture with mouse BMM. The Seven-day co-culture with BMM supported the formation of TRACP-positive multinucleated cells in both ST2 and C6 cells by FK (10^{-5} M) treatment; reflecting the high level of RANKL expressed in C6 cells by FK, the number of multinucleated cells supported by C6 cells was twice as high as that supported by ST2 cells (Fig. 1B left panel). By combined VitD and Dex treatment, however, C6 cells supported the formation of a nominal number of TRACP-positive multinucleated cells at a low dose (10^{-8} M) of VitD treatment; even at a high dose (10^{-7} M), formation of TRACP-positive multinucleated cells supported by C6 cells remained one fourth of that by ST2 cells (Fig. 1B middle panel). In C6 cells, the mRNA level of ATF-4, a major intracellular signaling machinery conveying FK treatment on the RANKL gene promoter through the CRE-like region at almost −0.96 kb [Elefteriou et al., 2005], was 42% higher than that of ST2 cells at steady state (Fig. 1B right panel). Photographs from the co-culture experiments are shown in Figure 1C.

Electrophoretic Motility Shift Assay (EMSA) and Site-Directed Mutagenesis Studies

Next, because mouse RANKL gene basic promoter has three putative Runx2-binding sites, we assessed the in vitro binding of nuclear protein from FK-treated ST2 cells to three putative Runx2-binding sites (Runx2-1: −378/−354, Runx2-2: −214/−194, Runx2-3: −200/−180) by EMSA. In each oligonucleotide, protein-DNA binding (arrowheads) at the putative-binding sites was observed and inhibited by the addition of excess amounts of cold competitors containing two consensus Runx2-binding sites (5′-CAGAACCAACCACAGGACCCAAACCACAGCCTCCAC-3′), which was supershifted with an anti-Runx2 antibody (Fig. 2A, arrows). Site-directed mutagenesis studies were then carried out to confirm that the obliteration of these putative Runx2-binding sites (Fig. 2B top panel illustrates three mutation constructs, mutRunx2-2, mutRunx2-2, 3, and mutRunx2-1, 2, 3) affected RANKL gene promoter activity. In ST2 cells, the basal activity of the 2 kb RANKL promoter decreased in all three mutation constructs, especially when the Runx2-2 and 3 sites were mutated (Fig. 2B, bottom left). Furthermore, mutation of all three Runx2-binding sites (pGL3-mutRunx2-1,2,3) nullified the inducible effect of FK on the exogenously transfected RANKL promoter. On the other hand, when transfected into Runx2-deficient C6 cells, these mutation constructs demonstrated no significant difference either with or without FK treatment. Moreover, the inducible effect of FK on RANKL promoter seen in ST2 cells remained nominal in C6 cells (Fig. 2B, bottom right).

The Involvement of CRE-Like Region in Conducting FK-Induced RANKL Promoter Activity

The basic promoter region of the *RANKL* gene contains a CRE-like region (−969/−962) partly shared with the vitamin D responsive element (VDRE) (Fig. 3A, top panel). To investigate whether the inducible effect of FK on the *RANKL* gene involves this CRE-like region, we examined the effect of deletion or site-directed mutagenesis on RANKL promoter activity by transient transfection studies. In both ST2 and C6 cells, FK (10^{-5} M) increased the activity of pGL3-1005 (containing 1 kb

upstream from transcription start site of the *RANKL* gene) to 200% of its basal level, and additional administration of H89, a specific inhibitor of PKA, decreased the activity to the basal level (Fig. 3B). On the other hand, FK did not affect the activity of pGL3-723, which lacks a CRE-like region in both ST2 and C6 cells. Additionally, in C6 cells, FK increased pGL3-2k activity by 40%, while it did not affect pGL3-mutCRE containing the mutated CRE-like sequence (TGAGGTCA to TGAGGAGG) (Fig. 3C). These data indicate that the positive

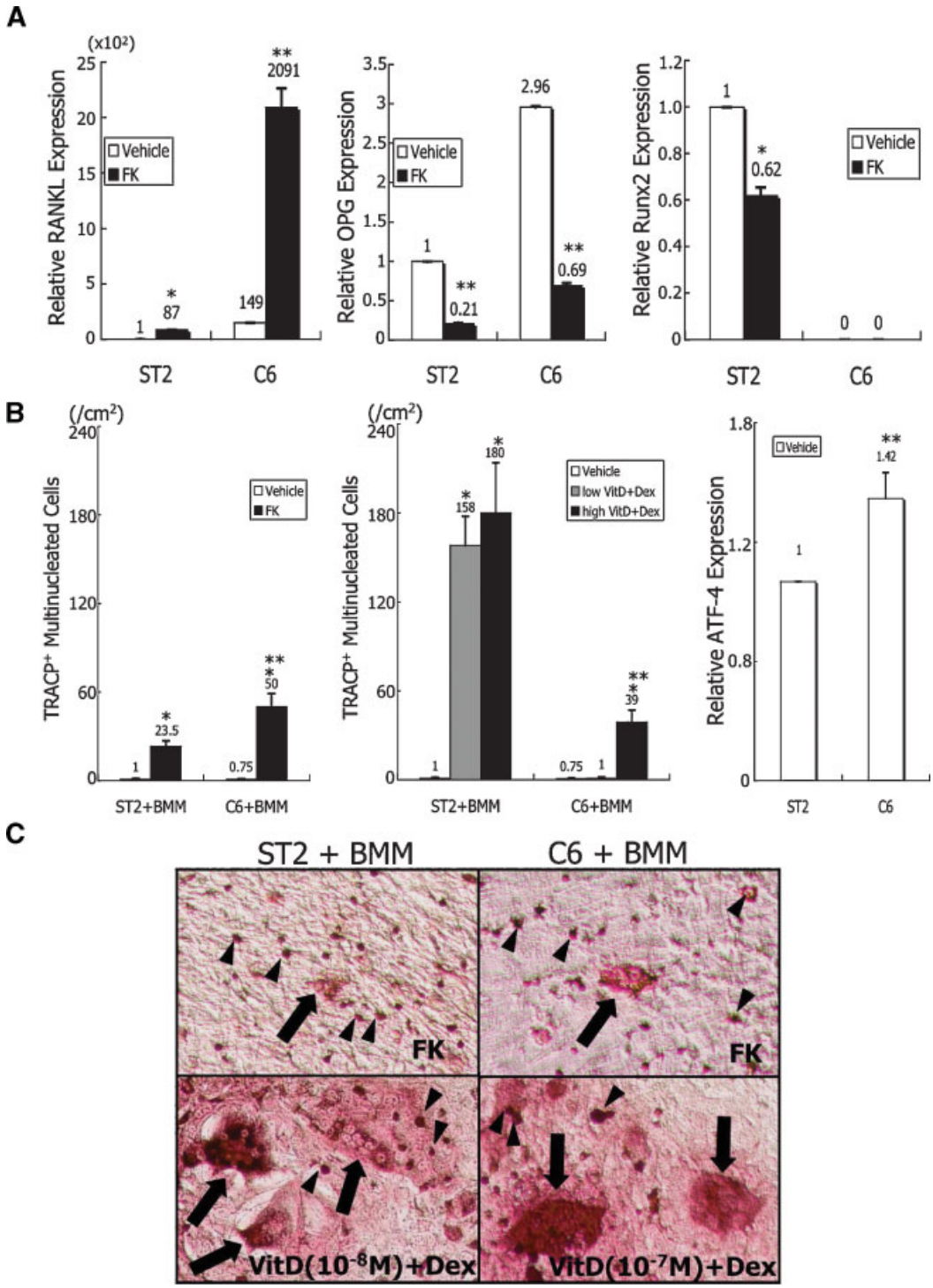

Fig. 1.

effect of FK on RANKL gene expression is conveyed through the CRE-like region of the basic promoter of RANKL. The inducible effect of FK on the exogenously transfected RANKL gene promoter, however, represented only part of the machinery compared with the enormous endogenous RANKL mRNA induction showing an 87 times increase in ST2 cells by FK treatment (Fig. 1A).

The Effect of Runx2 Knock-Down in ST2 Cells and of Forced Runx2 Expression in C6 Cells on RANKL Expression

The function of Runx2 in RANKL expression was confirmed through reducing the endogenous Runx2 mRNA expression in ST2 cells by small interfering RNA (siRNA). Runx2 knock-down by siRNA resulted in a significant decrease of Runx2 mRNA expression in ST2 cells to less than 30% of the control level (Fig. 4A, left panel). At the same time, mirroring the decrease of Runx2 expression, the steady-state expression of RANKL mRNA increased 1.54-fold by Runx2 knock-down. Moreover, the inducible effect of FK treatment in Runx2 knock-down ST2 cells diminished 56.8-fold, while control ST2 cells showed a 100.8-fold increase by FK treatment (Fig. 4A, right panel). Conversely, forced Runx2 expression in C6 cells using the Tet-On system showed restoration of the Runx2 protein in C6 cells by immunoblotting (Fig. 4B, top panel). Without FK stimulation, forced Runx2 expression in C6 cells decreased RANKL expression to 59% of the control level, while FK treatment increased RANKL expression in both Runx2 non-restored and restored C6 cells to 9.8- and 13.4-fold of the control level, respectively (Fig. 4B).

Histone H3 and H4 Acetylation/Phosphorylation Status in ST2 and C6 Cells

Next, since the inducible effect of FK on the exogenously transfected RANKL gene promoter accounted for only a part of the whole transcriptional machinery of the *RANKL* gene by FK, and since the exogenously transfected RANKL promoter construct did not show obvious differences in the luciferase activity between ST2 and C6 cells (Fig. 3B), the chromatin structure of the 5′-flanking region of the *RANKL* gene, especially histone modification, was assessed by the chromatin immunoprecipitation (ChIP) assay. Four sets of primers for post-immunoprecipitated DNA amplification were designed (Fig. 5A): one set of primers was set as far as −40 kb upstream of the RANKL gene transcription start site (a; −40.3 kb), and three (b; −26.6 kb, c; −12.7 kb, and d; −0.95/−0.68 kb) were set to cover the region within 1 kb downstream of the CRE site (−26.7 kb) or the CRE-like regions (−12.8 kb and −0.96 kb). In ST2 cells, histone acetylation was undetectable except for weak histone H3 acetylation in regions a and c without FK treatment. Upon FK treatment, histone H4 acetylation was observed in regions a and d (Fig. 5B). On the other hand, in C6 cells, histones H3 and H4 were acetylated regardless of FK treatment, indicating that the histone was constitutively acetylated over a wide range of the 5′-flanking region of the *RANKL* gene, in other words, in an open structure, in the steady-state (Fig. 5B). Phosphorylation of histone H3, however, showed no difference between control and FK-treated ST2 cells (Fig. 5C). Moreover, the level of the steady-state expression of HDAC3 in C6 cells was about half of that in ST2 cells, and it was

Fig. 1. RANKL, OPG, and Runx2 mRNA expression and osteoclastogenesis in ST2 and C6 cells. **A**: ST2 and C6 cells were treated with 10^{-5} M FK for 12 h, and then total RNA was extracted for quantitative real-time RT-PCR for RANKL, OPG, and Runx2. Administration of FK resulted in 87- and 14-fold increases of RANKL mRNA expression in ST2 and C6 cells, respectively. FK treatment decreased OPG expression to 20.9% and 24.2% of that in steady-state ST2 and C6 cells, respectively. In ST2 cells, FK decreased Runx2 expression to 59% of the basal expression, while C6 cells did not express Runx2. Results are expressed as the means ± SEM of the relative mRNA amount standardized by GAPDH from four cultures. (*$P < 0.05$ vs. vehicle, **$P < 0.001$ vs. vehicle.) (**B** left, middle, and **C**) ST2 or C6 cells were co-cultured with mouse bone marrow macrophages (BMM) for 7 days in the presence of 10^{-5} M FK, 10^{-8} M Dex, and 10^{-8} M (for ST2) or 10^{-7} M (for C6) VitD. B, left: TRACP-positive multinucleated cells (nucleus >3) were counted. FK caused a 23.5- and a 50-fold increase in the number of osteoclasts in ST2 and C6 cells, respectively. (*$P < 0.05$ vs. vehicle, **$P < 0.05$ vs. ST2 cells.) B, right: Steady-state expression of ATF-4 mRNA in both cell lines was measured by quantitative real-time RT-PCR. In C6 cells, the mRNA level of ATF-4 was 42% higher than that of ST2 cells at steady state (B, right panel). Results are expressed as the means ± SEM of the relative mRNA amount standardized by GAPDH from four cultures. (*$P < 0.05$ vs. ST2 cells.). C: Co-cultured cells were stained with TRACP. FK, as well as the combination of VitD and Dex, induced TRACP-positive mononucleated (arrowheads) and multinucleated (arrows) osteoclast-like cells in both ST2 and C6 cells.

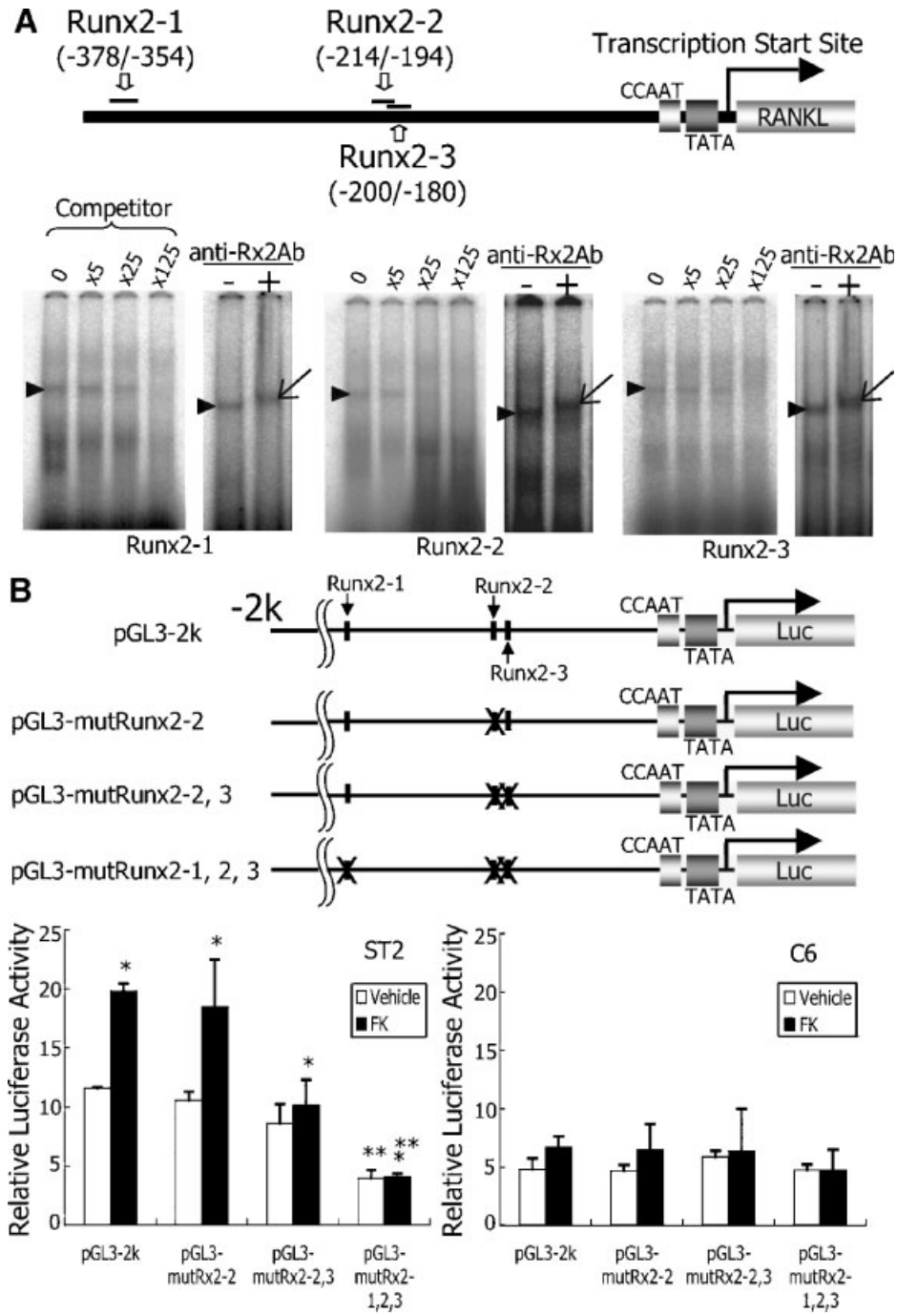

Fig. 2. EMSA and transient transfection studies using the mutations of Runx2-binding sites. **A**: In vitro binding of nuclear protein from FK-treated ST2 cells to three putative Runx2-binding sites (Runx2-1: −378/−354, Runx2-2: −214/−194, Runx2-3: −200/−180) was tested by EMSA. In each oligonucleotide, protein-DNA binding (arrowheads) at the putative-binding sites was observed and inhibited by the addition of excess amounts of cold competitors containing two consensus Runx2-binding sites (5′-CAGAACCAACCACAGGACCCAAACCACAGCCTCCAC-3′), which was supershifted with an anti-Runx2 antibody (anti-Rx2 Ab) (arrows). **B**: ST2 cells were transiently transfected with RANKL promoter-luciferase reporter gene construct pGL3-2k, and its mutated constructs (pGL3-mutRunx2-2, pGL3-mutRunx2-2,3, pGL3-mutRunx2-1,2,3). In ST2 cells, the mutation of Runx2-binding sites decreased the basal activity of the 2 kb RANKL promoter. Mutation of all three Runx2-binding sites (pGL3-mutRunx2-1,2,3) nullified the inducible effect of FK. On the other hand, in C6 cells, these mutations did not affect either basal or FK-induced promoter activity. Results are expressed as the means ± SEM of the relative luciferase activity standardized by phRG-TK promoter activity obtained from four cultures. (*$P < 0.05$ vs. vehicle, **$P < 0.05$ vs. pGL3-2k.)

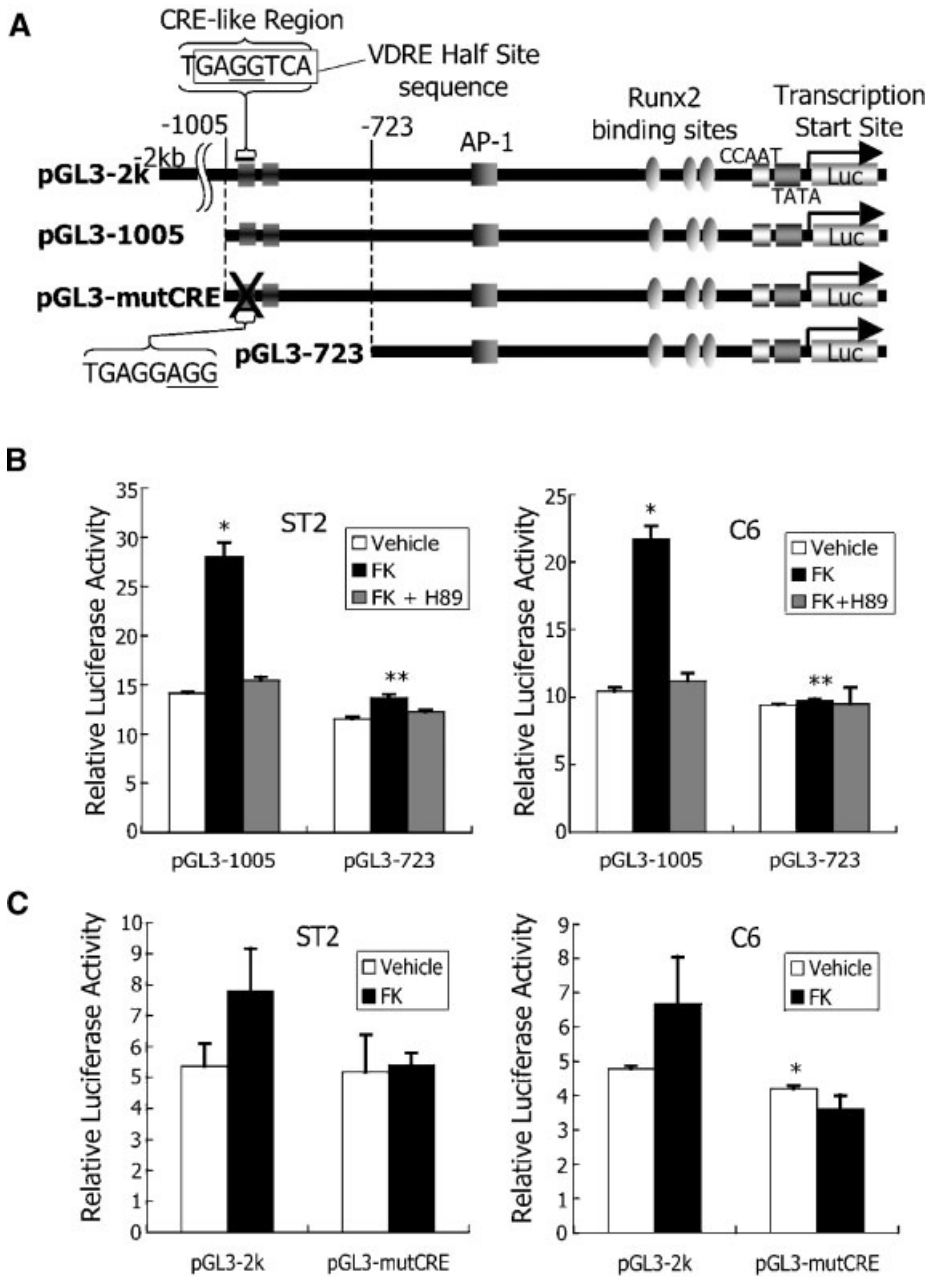

Fig. 3. Transient transfection studies using the mutants of the CRE-like site. **A**: The cyclic AMP responsive element (CRE)-like region is located at −969/−962 in the basic RANKL promoter. The promoter-reporter gene constructs with deletion or mutation (TGAGGTCA–TGAGGAGG) of the CRE-like site were generated. **B**: ST2 and C6 cells were transiently transfected with pGL3-1005 and pGL3-723, and then treated with FK alone or in combination with H89 for 12 h prior to the luciferase assay. In both ST2 and C6 cells, FK increased the activity of pGL3-1005 to 200% but did not affect that of pGL3-723. (*$P < 0.05$ vs. vehicle, **$P < 0.05$ vs. pGL3-1005.) **C**: FK increased the promoter activity of pGL3-2k to 140% in both ST2 and C6 cells, but did not affect that of pGL3-mutCRE. Results are expressed as the means ± SEM of the relative luciferase activity standardized by phRG-TK promoter activity obtained from four cultures. (*$P < 0.05$ vs. pGL3-2k.)

repressed to 40%–50% by FK treatment in both cells (Fig. 5D).

DISCUSSION

This study demonstrated that Runx2 suppressed steady-state RANKL gene expression by condensing the chromatin in osteoblastic cells and that FK transactivated the *RANKL* gene through the CRE-like site (−969/−962 bp) located in the RANKL gene promoter region and through the opening of the chromatin conformation by competing with Runx2 located

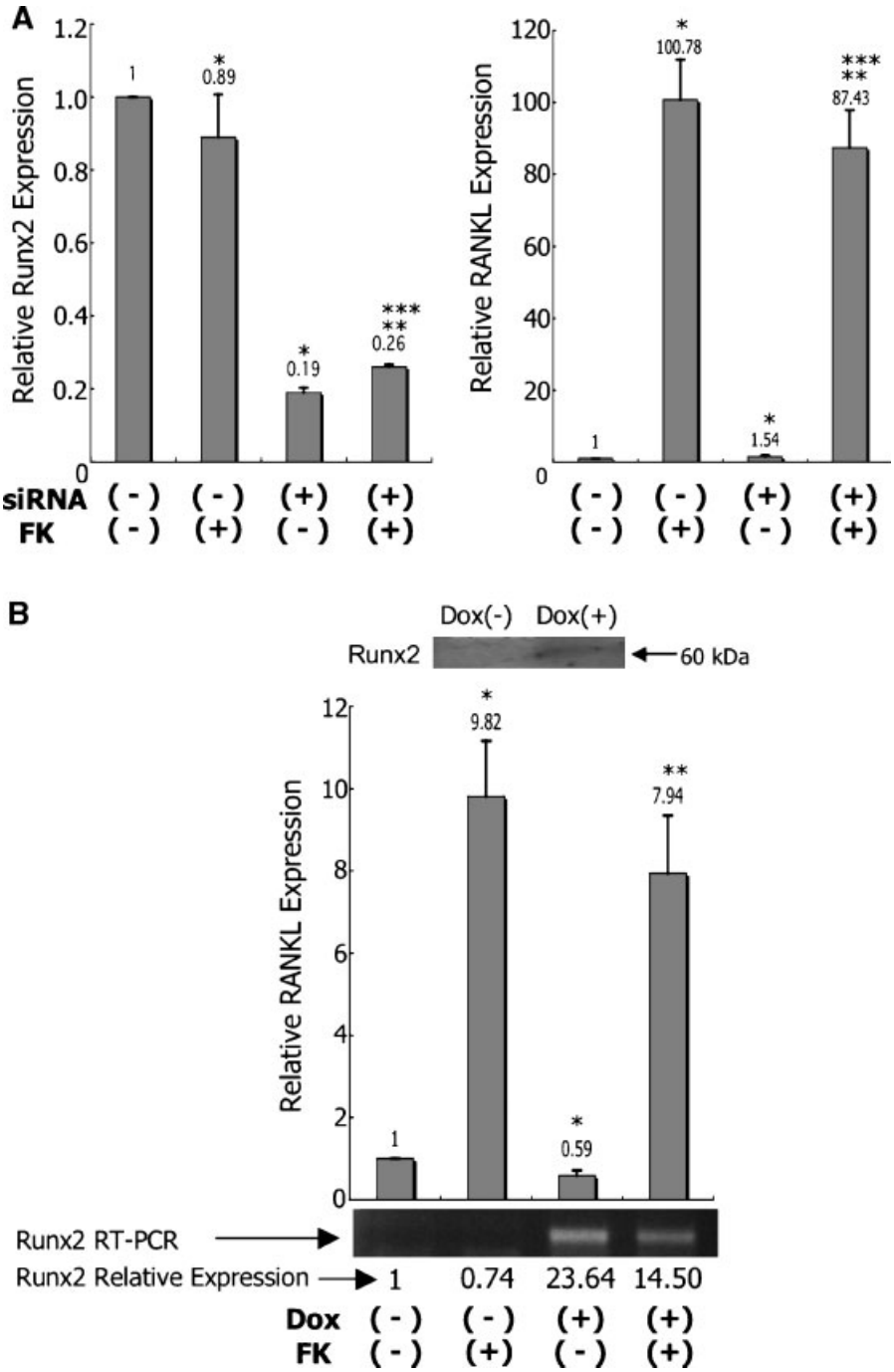

Fig. 4. The effect on RANKL expression of Runx2 knock-down in ST2 cells and of Runx2 restoration in C6 cells. **A**: Runx2 mRNA expression in ST2 cells was suppressed by siRNA (left). Runx2 knock-down increased RANKL mRNA expression at steady state by 1.5-fold, and decreased responsiveness to FK in RANKL expression from 100.8-fold to 56.8-fold (right). **B**: The top panel (immunoblotting) shows the Runx2 protein restoration in C6 cells by Tet-On system, and the bottom panel (RT-PCR) shows Runx2 mRNA. In C6 cells, Runx2 restoration decreased RANKL expression in the absence of FK treatment to 59% of its steady-state expression, and increased responsiveness to FK from 9.8-fold to 13.4-fold. Results are expressed as the means ± SEM of the relative mRNA amount standardized by GAPDH from four cultures. (*$P < 0.05$ vs. siRNA (−) and vehicle, **$P < 0.05$ vs. vehicle, and ***$P < 0.05$ vs. siRNA(−)).

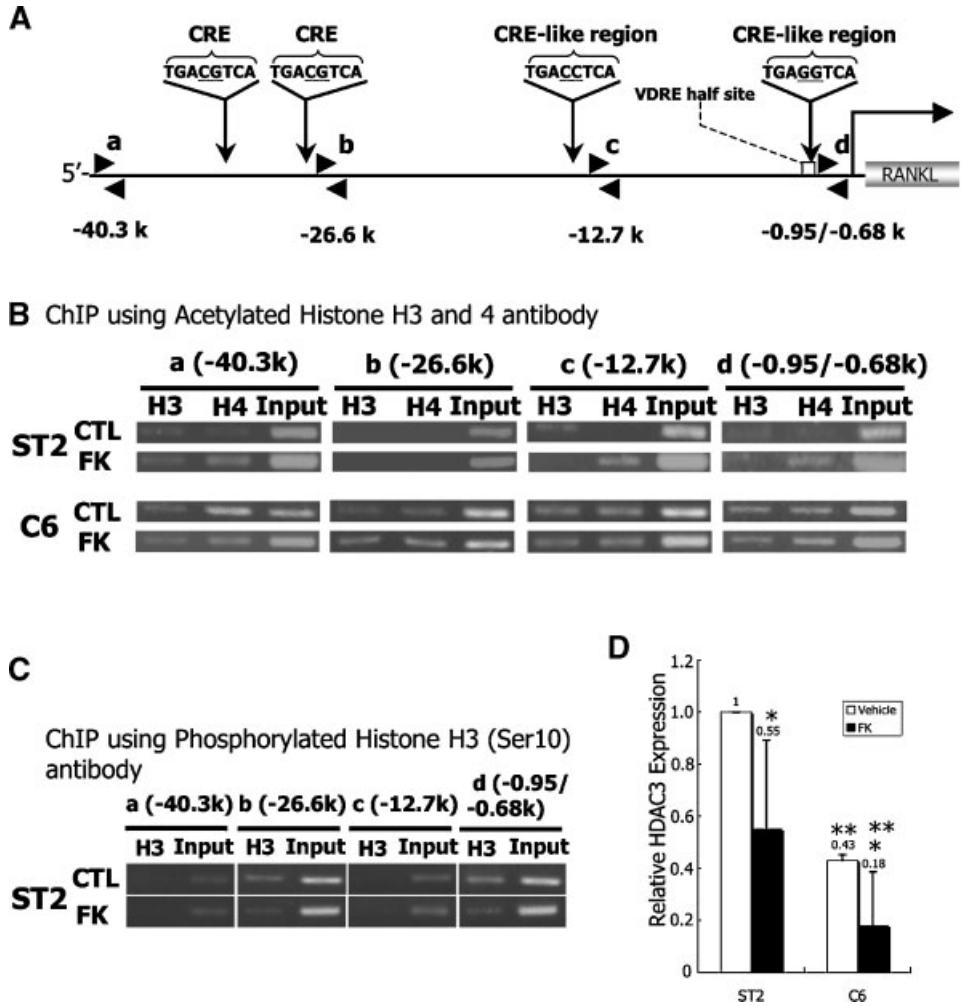

Fig. 5. Histone H3 and H4 acetylation/phosphorylation in response to FK. ST2 and C6 cells cultured with or without 10^{-5} M FK were subjected to chromatin immunoprecipitation (ChIP). Input and immunoprecipitated DNA with either anti-acetylated histone H3 or H4 antibodies (B) or anti-phosphorylated histone H3 (Ser 10) antibody (C) were assessed by PCR using four sets of primers (arrowheads) to amplify the regions described in panel (**A**). **B**: In ST2 cells, within and downstream of −26.6 kb, FK treatment induced H3 (b) and H4 (c, d) acetylation, while in C6 cells, regardless of FK treatment, H3 and H4 histone acetylation of all four regions was observed. **C**: In ST2 cells, FK treatment did not affect the phosphorylation of H3. **D**: HDAC3 mRNA expression in ST2 and C6 cells measured by quantitative real-time RT-PCR. The steady-state expression level in C6 cells was 42.8% of that in ST2 cells, and FK treatment repressed the expression level to 40%–50% in both cell lines. Results are expressed as the means ± SEM of the relative mRNA amount standardized by GAPDH from four cultures. (*$P < 0.05$ vs. vehicle, **$P < 0.05$ vs. ST2 cells.)

far upstream (more than −40 kb from the transcription start site) of the *RANKL* gene in osteoprogenitor cells.

Bone formation by endochondral ossification requires condensation of undifferentiated mesenchymal cells, followed by differentiation into hypertrophic chondrocytes, and by the mineralization of the surrounding cartilaginous matrices which are then resorbed by osteo(chondro)clasts, where extensive RANKL expression by hypertrophic chondrocytes is involved in the formation and activation of osteo(chondro)-clasts [Kawana and Sasaki, 2003; Takamoto et al., 2003; Kishimoto et al., 2005]. This endochondral ossification process is controlled by a member of the runt-homology gene family, Runx2 or Cbfa1. Because Runx2- and RANKL-expressing cells overlap in hypertrophic chondrocytes during endochondral ossification, Runx2 expression is speculated to be positively related to RANKL expression [Kishimoto et al., 2005]. While Runx2 positively induces the expression of the genes related to osteoblast-specific phenotypes such as type I collagen,

osteocalcin, and bone sialoprotein in osteoblast progenitors, it inhibits the terminal differentiation of osteoblasts at a later stage, indicating that the Runx2 transcription factor exerts diverse and controversial effects on osteoblastic cells, depending on their differentiation stage [Enomoto et al., 2003]. Indeed, after the establishment of mature trabecular bone, while mature osteoblastic cells continuously express Runx2 [Ducy et al., 1999], the steady-state expression of the *RANKL* gene is suppressed to a very low level [Komori, 2003]. Also, the ability of osteoprogenitor cells to support osteoclast formation decreases with their maturation stage [Manolagas, 2000]. We therefore speculate that Runx2 exerts an apparently opposite effect on RANKL gene expression depending on the stage of bone formation; in hypertrophic chondrocytes during endochondral ossification, Runx2 would positively control RANKL gene expression to recruit osteo(chondro)clasts for facilitating the endochondral ossification process by removing mineralized cartilaginous matrix, while after the establishment of mature trabecular bone, it would negatively regulate RANKL expression to sustain the established trabecular bone mass. We conducted our studies with the use of two artificial cell lines, ST2 and C6, both of which can be categorized as immature mesenchymal cell lines capable of differentiating into osteoblastic cells [Notoya et al., 2004].

By real-time RT-PCR, Runx2-deficient C6 cells showed a higher level of steady-state RANKL gene expression than did ST2 cells (Fig. 1A). Both cell lines responded to FK treatment and supported osteoclastogenesis in the coculture with BMM (Fig. 1B,C). In spite of the 23 times higher level of RANKL expression in C6 cells than in ST2 cells, the number of TRACP positive osteoclast-like cells supported by C6 cells was much smaller than that supported by FK-treated ST2 cells. A relatively high level of OPG, a decoy receptor for RANKL, in C6 cells even after FK treatment probably accounts for this low efficiency of osteoclastogenesis by C6 cells, as in the case of the low dose of VitD [Notoya et al., 2004], while the difference of the efficiency of osteoclastogenesis between C6 and ST2 cells may be partly attributable to the difference in the expression status of their macrophage-colony stimulating factor (M-CSF). We therefore speculated that Runx2 exerted a negative effect on steady-state RANKL gene expression in osteoblast/stromal cell lines, simulating the late stage of endochondral ossification where steady-state RANKL gene expression is kept at a low level after the removal of cartilaginous tissue by osteo(chondro)clasts.

In general, Runx2 modulates bone-related genes through two major mechanisms. First, Runx2 directly affects target genes containing Runx2-binding elements in their promoters [Ji et al., 1998; Drissi et al., 2000]. Alternatively, by recruiting histone-modifying enzymes such as histone deacetylase (HDAC) 3, 4, and 6, Runx2 modulates gene expression by changing the chromatin structure [Westendorf et al., 2002; Schroeder et al., 2004; Vega et al., 2004; Liu et al., 2005]. The mouse RANKL gene basic promoter region contains three putative Runx2-binding sites, suggesting the involvement of Runx2 in bone-specific RANKL expression [Kitazawa et al., 1999]. EMSA using nuclear extracts from ST2 cells, interfering with competitors including two consensus Runx2-binding sites, showed specific bindings between a nuclear protein and these three putative-binding sites, indicating that the Runx2 protein can bind to these three putative Runx2-binding sites in vitro (Fig. 2A). Moreover, site-directed mutagenesis studies demonstrated that the deprivation of the Runx2-binding sites slightly downregulated RANKL gene promoter activity. The effect was most prominent and reduced to 40% from its original activity when all three Runx2-binding sites were mutated. Such reduction of the promoter activity was not observed in Runx2-null C6 cells (Fig. 2B). Although we must admit that the impact of direct Runx2 binding to the exogenously transfected RANKL gene promoter region remained minimal [as has been reported by O'Brien et al., 2002] through these three Runx2-binding sites in the RANKL gene promoter, Runx2 exerts a modest but positive effect on promoter activity. FK treatment, on the other hand, positively regulated RANKL gene promoter activity, which was not affected much by the deprivation of the Runx2-binding sites. These data indicate that FK treatment, besides downregulating the Runx2 expression level in ST2 cells to 60% (Fig. 1A, right panel), affects the exogenously transfected RANKL gene promoter activity mostly through a Runx2-independent mechanism.

Next, to investigate the Runx2-independent mechanism by which FK treatment affected

the exogenously transfected RANKL gene promoter activity, we carried out deletion or site-directed mutagenesis studies focused on the CRE-like region (−969/−962 bp) partly shared by VDRE (−968/−962 bp) (Fig. 3A). Because addition of a PKA inhibitor, H89, and deletion (Fig. 3B) and mutation (Fig. 3C) of the CRE-like region almost completely nullified the inducible effect of FK on exogenously transfected RANKL gene promoter activity, we reasoned that activation of the promoter by FK treatment is mediated mainly through this CRE-like region. The FK-induced activation of the luciferase construct was not of great influence, but it partly explains the prominent fold induction of endogenous RANKL mRNA in ST2 cells.

To confirm that Runx2 negatively regulates the steady-state expression of the endogenous *RANKL* gene, we inhibited Runx2 expression by siRNA (Fig. 4A) in ST2 cells, and conversely, forced the induction of Runx2 by the Tet-On vector system (Fig. 4B) in C6 cells. In both systems, a reciprocal pattern between Runx2 and RANKL gene expression was observed, and FK upregulated RANKL gene expression irrespective of the Runx2 level. Nonetheless, a discrepancy was observed between the level of endogenous RANKL gene expression and exogenous transfected RANKL promoter activity in response to FK treatment. We therefore explored the chromatin remodeling mechanism by which Runx2 and FK treatment regulate

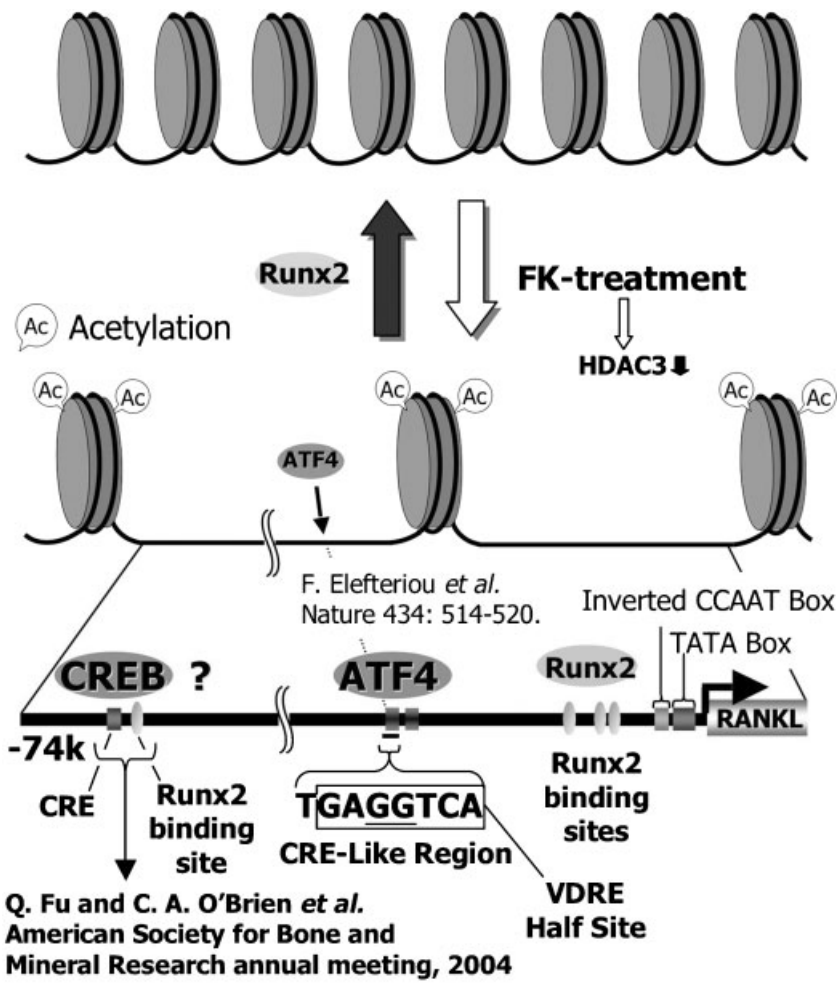

Fig. 6. A model by which Runx2 and the CRE-binding protein (CREB) regulate RANKL expression. In ST2 cells, first, Runx2 and FK treatment regulate RANKL gene expression in a reciprocal manner through chromatin remodeling. Induction of ATF-4 and reduction of HDAC3 promote acetylation of histone H3 or H4 and trigger chromatin relaxation, while Runx2 induces chromatin condensation. By FK treatment, because of chromatin relaxation, transcription factors can approach the basic promoter region of the *RANKL* gene. Runx2 plays a role in condensing chromatin to suppress the gene; at the same time, however, Runx2 is potentially capable of promoting gene expression through these Runx2-binding sites at the basic promoter region.

RANKL gene expression. By searching the database with the GENETYX-MAC software package (ver. 10) (GENETYX, Tokyo, Japan), we identified three putative CRE sites at 31.8, 26.8, and 13.2 kb upstream of the *RANKL* gene (Fig. 5A) and examined the acetylation status of these areas by ChIP assay (Fig. 5B). Runx2-deficient C6 cells showed H3 and H4 histone acetylation, and thereby the opening of the chromatin structure at least as far as 40.3 kb upstream of the *RANKL* gene in the steady state. Additionally, FK treatment increased the acetylated H4 histone at −0.96 kb in both ST2 and C6 cells and slightly at −40.3 and −12.7 kb in ST2 cells. These data suggest that Runx2 plays a role in condensing chromatin to suppress the *RANKL* gene, and that FK treatment antagonizes the function of Runx2 on RANKL gene expression by reducing the level of Runx2 mRNA expression and by opening the chromatin structure far upstream (more than 40 kb) from the *RANKL* gene. Indeed, solitary Runx2 is incapable of chromatin remodeling [Young et al., 2005]. Runx2 can recruit factors that are capable of chromatin remodeling activity [Westendorf et al., 2002; Schroeder et al., 2004], to the specific Runx2-target gene in osseous cells. Most important, Runx2 interacts with HDAC3 and represses osteocalcin gene expression in osteoblastic cells [Schroeder et al., 2004]. Since the RANKL gene promoter shares structural similarities with osteocalcin and bone sialoprotein [Kitazawa et al., 1999], we hypothesized that Runx2 plays a similar role in RANKL gene expression. We found that Runx2 deficiency per se and FK treatment reduced HDAC3 mRNA level in ST2 and C6 cells (Fig. 5D). Consequently, Runx2 deficiency and FK treatment accelerate histone acetylation by competing with Runx2, and by reducing HDAC3 itself.

Furthermore, FK, per se, transactivates the *RANKL* gene through the CRE-like region at −0.96 kb. Recently, Fu et al. [2004] have reported the presence of the conserved DNA structure where Runx2 and CRE are closely located 74 kb upstream of the *RANKL* gene (Fig. 6). We therefore propose a model by which Runx2 and FK regulate RANKL expression (Fig. 6). The expression profile of Runx2-associating co-activators and co-repressors [Lian et al., 2003; Schroeder et al., 2004], especially histone-modifying enzymes, during the endochondral ossification process or during osteoblast differentiation may explain the apparent controversial effects of Runx2 on RANKL gene expression.

ACKNOWLEDGMENTS

This work was supported in part by a Grant-in-Aid for Scientific Research from the Ministry of Education, Culture, Sports, Science and Technology, Japan, (16590278 to S.K. and 16590313 to R.K.). The authors thank Dr. Agus Darwanto for scientific contribution, and Mr. Shuichi Matsuda and Ms. Noriko Sakamoto for excellent technical assistance.

REFERENCES

Boyle WJ, Simonet WS, Lacey DL. 2003. Osteoclast differentiation and activation. Nature 423:337–342.

Drissi H, Luc Q, Shkoori R, Chuva de Sousa Lopes S, Choi JY, Terry A, Hu M, Jones S, Neil JC, Lian JB, Stein JL, van Wijnen AJ, Stein GS. 2000. Transcriptional autoregulation of the bone related *CBFA1/RUNX2* gene. J Cell Physiol 181:314–350.

Ducy P, Zhang R, Geoffory V, Ridall AL, Karsenty G. 1997. Osf2/Cbfa1: A transcriptional activator of osteolast differentiation. Cell 89:747–754.

Ducy P, Starvuck M, Priemel M, Shen J, Pinero G, Geoffroy V, Amling M, Karsenty G. 1999. A Cbfa1-dependent genetic pathway controls bone formation beyond embryonic development. Genes Dev 13:1025–1036.

Ducy P, Schinke T, Karsenty G. 2000. The osteoblast: A sophisticated fibroblast under central surveillance. Science 289:1501–1504.

Elefteriou F, Ahn JD, Takeda S, Starbuck M, Yang X, Liu X, Kondo H, Richards WG, Bannon TW, Noda M, Clement K, Vaisse C, Karsenty G. 2005. Leptin regulation of bone resorption by the sympathetic nervous system and CART. Nature 434:514–520.

Enomoto H, Shiojiri S, Hoshi K, Furuichi T, Fukuyama R, Yoshida CA, Kanatani N, Nakamura R, Mizuno A, Zanma A, Yano K, Yasuda H, Higashio K, Takada K, Komori T. 2003. Induction of osteoclast differentiation by Runx2 through receptor activator of nuclear factor-κB ligand (RANKL) and osteoprotegerin regulation and partial rescue of osteoclastogenesis in $Runx2^{-/-}$ mice by RANKL transgene. J Biol Chem 278:23971–23977.

Fu Q, Foote LP, Manolagas SC, O'Brien CA. 2004. An evolutionarily conserved CREB-binding enhancer, in an unusually remote location 74 kb upstream from the initiation site, confers the stromal/osteoblast-specific control of RANKL transcription by PTH, $1,25(OH)_2D_3$, and gp130 cytokines. J Bone Miner Res 19(suppl 1):s28.

Geoffroy V, Kneissel M, Fournier B, Boyde A, Matthias P. 2002. High bone resorption in adult aging transgenic mice overexpressing Cbfa1/Runx2 in cells of the osteoblastic lineage. Mol Cell Biol 22:6222–6233.

Ji C, Casinghino S, Chang DJ, Chen Y, Javed A, Ito Y, Hiebert SW, Lian JB, Stein GS, McCarthy TL, Centrella M. 1998. CBFa(AML/PEBP2)-related elements in the TGF-β type I receptor promoter and expression with osteoblast differentiation. J Cell Biochem 69: 353–363.

Kania MA, Bonner AS, Duffy JB, Gergen JP. 1990. The *Drosophila* segmentation gene runt encodes a novel nuclear regulatory protein that is also expressed in the developing nervous system. Genes Dev 4:1701–1713.

Kawana F, Sasaki T. 2003. Osteoclast differentiation and characteristic trabecular bone formation during growth plate destruction in osteoprotegerin-dificient mice. J Electron Microsc (Tokyo) 52:515–525.

Kern B, Shen J, Starbuck M, Karsenty G. 2001. Cbfa1 contributes to the osteoblast-specific expression of type I collagen genes. J Biol Chem 276:7101–7107.

Kishimoto K, Kitazawa R, Kurosaka M, Maeda S, Kitazawa S. 2005. Expression profile of genes related to osteoclastogenesis in mouse growth plate and articular cartilage. Histochem Cell Biol (in press).

Kitazawa R, Kitazawa S. 2002. Vitamin D_3 augments osteoclastogenesis via Vitamin D-responsive element of mouse *RANKL* gene promoter. Biochem Biophys Res Commun 290:650–655.

Kitazawa S, Ross FP, McHugh K, Teitelbaum SL. 1995. Interleukin-4 induces expression of the integrin $\alpha_v\beta_3$ via transactivation of the β_3 gene. J Biol Chem 270:4115–4120.

Kitazawa R, Kitazawa S, Maeda S. 1999. Promoter structure of mouse *RANKL*/*TRANCE*/*OPG*/*ODF* gene. Biochem Biopys Acta 1445:134–141.

Komori T. 2003. Requisite roles of Runx2 and Cbfb in skeletal development. J Bone Miner Metab 21:193–197.

Komori T, Yagi H, Nomura S, Yamaguchi A, Sakai K, Deguchi K, Shimizu Y, Bronson RT, Gao YH, Inada M, Sato M, Okamoto R, Kitamura Y, Yoshiki S, Kishimoto T. 1997. Target disruption of Cbfa1 results in a complete lack of bone formation owing to maturational arrest of osteoblasts. Cell 89:755–764.

Kondo T, Kitazawa R, Maeda S, Kitazawa S. 2004. 1α,25 dihydroxyvitamin D_3 rapidly regulates the mouse osteoprotegerin gene through dual pathways. J Bone Miner Res 19:1411–1419.

Lacy DL, Timms E, Tan HL, Kelley MJ, Dunstan CR, Burgess T, Elliott R, Colombero A, Elliott G, Scully S, Hsu H, Sullivan J, Hawkins N, Davy E, Capparelli C, Eli A, Qian YX, Kaufman S, Sarosi I, Shalhoub V, Senaldi G, Guo J, Delaney J, Boyle WJ. 1998. Osteoprotegerin ligand is a cytokine that regulates osteoclast differentiation and activation. Cell 93:165–176.

Lian JB, Stein JL, Stein GS, van Wijnen AJ, Montecino M, Javed A, Gutierrez S, Shen J, Zaidi SK, Drissi H. 2003. Runx2/Cbfa1 functions: Diverse regulation of gene transcription by chromatin remodeling and co-regulatory protein interactions. Connect Tissue Res 44(suppl 1):141–148.

Liu W, Toyosawa S, Furuichi T, Kanatani N, Yoshida C, Liu Y, Himeno M, Narai S, Yamaguchi A, Komori T. 2001. Overexpression of Cbfa1 in osteoblasts inhibits osteoblast maturation and causes osteopenia with multiple fractures. J Cell Biol 155:157–166.

Liu C, Chang E, Yu J, Carlson CS, Prazak L, Yu XP, Ding B, Lengyel P, Cesare PED. 2005. The interferon-inducible p204 protein acts as a transcriptional coactivator of Cbfa1 and enhances osteoblast differentiation. J Biol Chem 280:2788–2796.

Manolagas SC. 2000. Birth and death of bone cells: Basic regulatory mechanisms and implications for the pathogenesis and treatment of osteoporosis. Endocr Rev 21:115–137.

Nakagawa N, Kinosaki M, Yamaguchi K, Shima N, Yasuda H, Yano K, Morinaga T, Higashio K. 1998. RANK is the essential signaling receptor for osteoclast differentiation factor in osteoclastogenesis. Biochem Biophys Res Commun 253:395–400.

Notoya M, Otsuka E, Yamaguchi A, Hagiwara H. 2004. Runx-2 is not essential for the Vitamin D-regulated expression of RANKL and osteoprotegerin in osteoblastic cells. Biochem Biophys Res Commun 324:655–660.

O'Brien CA, Kern B, Gubrij I, Karsenty G, Manolagas C. 2002. Cbfa1 does not regulate *RANKL* gene activity in stromal/osteoblasic cells. Bone 30:453–462.

Ogawa E, Maruyama M, Kagoshima H, Inuzuka M, Lu J, Satake M, Shigesada K, Ito Y. 1993. PEBP2/PEA2 represents a family of transcription factors homologous to the products of the *Drosophila* runt gene and the human *AML1* gene. Proc Natl Acad Sci USA 90:6859–6863.

Otto F, Thornell AP, Crompton T, Denzel A, Gilmour KC, Rosewell IR, Stamp GWH, Beddington RSP, Mundlos S, Olsen BR, Selby PB, Owen MJ. 1997. Cbfa1, a candidate gene for cleidocranial dysplasia syndrome, is essential for osteoblast differentiation and bone development. Cell 89:765–771.

Roca H, Phimphilai M, Gopalakrishnan R, Xiao G, Franceschi RT. 2005. Cooperative interactions between Runx2 and homeodomain protein binding sites are critical for the osteoblast-specific expression of the bone sialoprotein gene. J Biol Chem 280:30845–30855.

Schroeder TM, Kahler RA, Li X, Westendorf JJ. 2004. Histone deacetylase 3 interacts with Runx2 to repress the osteocalcin promoter and regulate osteoblast differentiation. J Biol Chem 279:41998–42007.

Suda T, Takahashi N, Udagawa N, Jimi E, Gillespie MT, Martin TJ. 1999. Modulation of osteoclast differentiation and function by the new members of the tumor necrosis factor receptor and ligand families. Endocr Rev 20:345–357.

Takahashi N, Akatsu T, Udagawa N, Sasaki T, Yamaguchi A, Moseley JM, Martin TJ, Suda T. 1988. Osteoblastic cells are involved in osteoclast formation. Endocrinology 123:2600–2602.

Takami M, Takahashi N, Udagawa N, Miyaura C, Suda K, Woo JT, Martin TJ, Nagai K, Suda T. 2000. Intracellular calcium and protein kinase C mediate expression of receptor activator of nuclear factor-κB ligand and osteoprotegerin in osteoblasts. Endocrinology 141:4711–4719.

Takamoto M, Tsuji K, Yamashita T, Sasaki H, Yano T, Taketani Y, Komori T, Nifuji A, Noda M. 2003. Hedgehog signaling enhances core-binding factor a1 and receptor activator of nuclear factor-κB ligand (*RANKL*) gene expression in chondrocytes. J Endocrinol 177:413–421.

Teitelbaum SL. 2000. Bone resorption by osteoclasts. Science 289:1504–1508.

Teitelbaum SL, Ross FP. 2003. Genetic regulation of osteoclast development and function. Nature Rev Genet 4:638–649.

Udagawa N, Takahashi N, Akatsu T, Sasaki T, Yamaguchi A, Kodama H, Martin TJ, Suda T. 1989. The bone marrow-derived stromal cell lines MC3T3-G2/PA6 and ST2 support osteoclast-like cell differentiation in coculture with mouse spleen cells. Endocrinology 125:1805–1813.

Vega RB, Matsuda K, Oh J, Barbosa AC, Yang X, Meadows E, McAnally J, Pomajzl C, Shelton JM, Richardson JA, Karsenty G, Olson EN. 2004. Histone deacetylase 4 controls chondrocyte hypertrophy during skeletogenesis. Cell 119:555–566.

Westendorf JJ, Zaidi SK, Cascino JE, Kahler R, van Wijnen AJ, Lian JB, Yoshida M, Stein GS, Li X. 2002. Runx2 (Cbfa1, AML-3) interacts with histone deacetylase 6 and represses the $p21^{CIPI/WAF1}$ promoter. Mol Cell Biol 22:7982–7992.

Xiao G, Jiang D, Ge C, Zhao Z, Lai Y, Boules H, Phimphilai M, Yang X, Karsenty G, Franceschi RT. 2005. Cooperative interactions between ATF4 and Runx2/Cbfa1 stimulate osteoblast-specific osteocalcin gene expression. J Biol Chem 280:30689–30696.

Yamaguchi A, Komori T, Suda T. 2000. Regulation of osteoblast differentiation mediated by bone morphogenetic proteins, hedgehogs, and Cbfa1. Endocr Rev 21: 393–411.

Yasuda H, Shima N, Nakagawa N, Yamaguchi K, Kinosaki M, Mochizuki S, Tomoyasu A, Yano K, Goto M, Murakami A, Tsuda E, Morinaga T, Higashio K, Udagawa N, Takahashi N, Suda T. 1998. Osteoclast differentiation factor is a ligand for osteoprotegerin/osteoclastogenesis-inhibitory factor and is identical to TRANCE/RANKL. Proc Natl Acad Sci USA 95:3597–3602.

Yoshida CA, Furuichi T, Fujita T, Fukuyama R, Kanatani N, Kobayashi S, Satake M, Takada K, Komori T. 2002. Core-binding factor β interacts with Runx2 and is required for skeletal development. Natrure Genet 32:633–638.

Young DW, Pratap J, Javed A, Weiner B, Ohkawa Y, van Wijnen A, Montecino M, Stein GS, Stein JL, Imbalzano AN, Lian JB. 2005. SWI/SNF chromatin remodeling complex is obligatory for BMP2-induced, Runx2-dependent skeletal gene expression that controls osteoblast differntiation. J Cell Biochem 94:720–730.